Chemosphere 286 (2022) 131637

Contents lists available at ScienceDirect

Chemosphere

journal homepage: www.elsevier.com/locate/chemosphere

Monitoring morphological changes from activated sludge to aerobic granular sludge under distinct organic loading rates and increasing minimal imposed sludge settling velocities through quantitative image analysis

Sérgio A. Silva [a], Angeles Val del Río [b], António L. Amaral [c], Eugénio C. Ferreira [a], M. Madalena Alves [a], Daniela P. Mesquita [a,*]

[a] CEB - Centre of Biological Engineering, Universidade do Minho, Campus de Gualtar, 4710-057, Braga, Portugal
[b] CRETUS Institute, Department of Chemical Engineering, Universidade de Santiago de Compostela, E, 15705, Santiago de Compostela, Spain
[c] Instituto Politécnico de Coimbra, ISEC, Rua Pedro Nunes, Quinta da Nora, 3030-199, Coimbra, Portugal

HIGHLIGHTS

- QIA is a suitable tool to access aerobic sludge granulation rates.
- The morphology of small granules reflected the degree of sludge aggregation.
- Principal component analysis allowed to discriminate the granulation process.
- SVI_5 and SVI_{30} were successfully predicted by partial least square regression.
- The sludge morphological changes correlated best with the SVI_5.

GRAPHICAL ABSTRACT

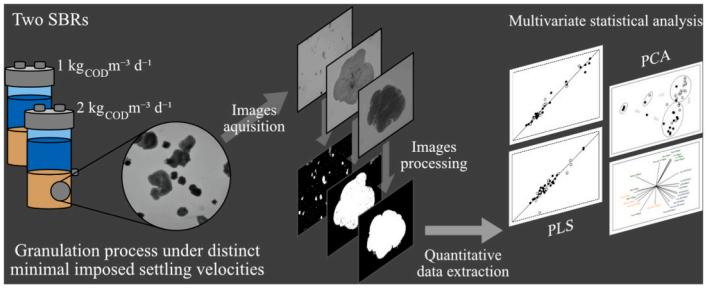

ARTICLE INFO

Handling Editor: A Adalberto Noyola

Keywords:
Aerobic granulation process
Sequencing batch reactors
Image processing
Partial least squares
Principal component analysis

ABSTRACT

Quantitative image analysis (QIA) was used for monitoring the morphology of activated sludge (AS) during a granulation process and, thus, to define and quantify, unequivocally, structural changes in microbial aggregates correlated with the sludge properties and granulation rates. Two sequencing batch reactors fed with acetate at organic loading rates of 1.1 ± 0.6 kg_{COD} m^{-3} d^{-1} (R1) and 2.0 ± 0.2 kg_{COD} m^{-3} d^{-1} (R2) and three minimal imposed sludge settling velocities (0.27 m h^{-1}, 0.53 m h^{-1}, and 5.3 m h^{-1}) induced distinct granulation processes and rates. QIA results evidenced the turning point from flocculation to granulation processes by revealing the differences in the aggregates' stratification patterns and quantifying the morphology of aggregates with equivalent diameter (Deq) of 200 μm ≤ Deq ≤ 650 μm. Multivariate statistical analysis of the QIA data allowed to distinguish the granulation status in both systems, by clustering the observations according to the sludge aggregation and granules maturation status, and successfully predicting the sludge volume index measured at 5 min (SVI_5) and 30 min (SVI_{30}). These results evidence the possibility of defining unequivocally the granulation rate and anticipating the sludge settling properties at early stages of the process using QIA data. Hence, QIA could be used to predict episodes of granules disruption and hindered settling ability in aerobic granulation sludge processes.

* Corresponding author.
E-mail address: daniela@deb.uminho.pt (D.P. Mesquita).

https://doi.org/10.1016/j.chemosphere.2021.131637
Received 11 March 2021; Received in revised form 20 July 2021; Accepted 20 July 2021
Available online 24 July 2021

1. Introduction

The aerobic granular sludge (AGS) is a breakthrough technology, with a tremendous potential to become the new standard for aerobic treatment of wastewater, due to its compact design and lower footprint. Synthetic media and real wastewaters have been used to produce granules from activated sludge in sequencing batch reactors (SBR) (Carrera et al., 2019; Devlin et al., 2017; Li et al., 2008; Liu et al., 2017; Morgenroth et al., 1997; Sguanci et al., 2019). The process of granules formation, i.e. granulation, is generally described as a stepwise process, triggered by certain environmental conditions (Liu and Tay, 2002; Wilén et al., 2018). In lab-scale SBR, granulation can occur within few weeks, however, it may vary depending on the type of substrate (Pronk et al., 2015a), operating conditions (Rollemberg et al., 2019), and the presence of recalcitrant compounds (Jiang et al., 2021).

Nevertheless, the long start-up periods needed to obtain mature granules, and their stability, are still concerns of the AGS technology. This is particularly observed in scale-up studies. For instance, Liu et al. (2010) reported that the predominance of granules was only achieved after 400 days, in a pilot-scale SBR used to treat a mixture of domestic and industrial wastewater. Also, Pronk et al. (2015b) reported that a start-up period of 5 months was necessary to achieve stable granules in a full-scale AGS plant treating domestic wastewater. Wagner et al. (2015) reported that the granulation process in the presence of particulate organic matter was slower than with readily biodegradable soluble substrate, and that a substantial flocs fraction always remained in the system. More recently, Xavier et al., (2021) achieved a granular fraction of over 80 % in less than 3 months in a pilot-scale reactor fed with low strength domestic wastewater. However, the granular fraction could not be maintained throughout the reactor operation. Therefore, although complete conversion from conventional activated sludge (CAS) to AGS is often reported in lab-scale studies, the coexistence of floccular and granular fractions in pilot- and full-scale AGS systems is observed, even after the granulation start-up period (Liu et al., 2010; Pronk et al., 2015b; Xavier et al., 2021). This floccular sludge is particularly critical for the clarification process.

The qualitative characterization, by visual inspection, of granular sludge transitioning from CAS to granules is rather subjective and pales in importance to the ratio SVI_{30}/SVI_5 of the sludge volume index measured at 5 min (SVI_5) and 30 min (SVI_{30}). This parameter is commonly used to monitor SBR granulation status (Liu and Tay, 2007), though similar SVI_{30} and SVI_5 values can occur in a flocs dominated sludge (Liu et al., 2010) compared to a granular dominated sludge, making the SVI on its own unfit to monitor the granulation status. Several authors defined the percentage of aggregates larger than 200 μm in equivalent diameter (Deq) as an indicator of the granules percentage in aerobic reactors, given that de Kreuk et al. (2007) defined this size as the minimal size of granules. However, more detailed morphological information, specifically related with the aggregated biomass dynamic changes and filamentous bacteria, is found useful during sludge granulation in SBR start-up periods, being relevant to increase the knowledge about the rates and stability of the AGS formed under defined operating conditions.

Quantitative image analysis (QIA) is a powerful monitoring tool to quantify morphological changes of sludge aggregates in both aerobic (Mesquita et al., 2011a) and anaerobic treatment processes (Amaral et al., 2004; Araya-Kroff et al., 2004). In these studies, it was possible to assess disturbances in CAS systems, as well as quantify morphological changes during anaerobic granulation and deterioration in an expanded granular sludge blanket reactor (EGSB) reactor using QIA. Recently, the effect of pharmaceutical active compounds on mature aerobic granules was assessed trough QIA (Leal et al., 2021a, 2021b). In aerobic granulation studies, Beun et al. (2002) determined the diameter, aspect ratio and shape factor of granules formed using QIA and reported that the aspect ratio and shape factor stabilized prior to the average diameter. Also, the granules formation process in a SBR treating soybean processing wastewater was described by QIA (Su and Yu, 2005). These authors suggested that the decrease of the granules roundness and aspect ratio evidenced that the flocs evolved gradually to dense, regular and round aggregates induced by detachment of loosely adhered microorganism under high shear forces (Su and Yu, 2005). However, in these works, solely a small number of parameters were used to describe the granulation process and quantitative information about the flocs and filaments was limited or non-existent. It has been suggested that filamentous bacteria could generate structural support to initiate granules formation (Zhang et al., 2011), with the possibility of measuring the length of free and protruding filamentous bacteria being a powerful feature of QIA in this context. In addition, the presence of filamentous growth on anaerobic sludge bed has already been quantified during detergent shock loads, in order to act as an early warning indicator of sludge washout in anaerobic digesters (Costa et al., 2007).

Coupling operational data, from biological treatment systems, with the large amount of data provided by QIA in sludge characterization, requires the use of multivariable statistical techniques to extract the most relevant information and properly monitor these systems. Multivariable statistical techniques, such as principal component analysis (PCA) and partial least squares (PLS), have been applied successfully to QIA data to predict the effect of toxic loads in anaerobic granular sludge (Costa et al., 2009) and to predict the effluent quality in CAS systems (Mesquita et al., 2016). Recently, SVI_{30} of mature aerobic granules could be predicted using a multivariable statistical technique with QIA data (Leal et al., 2020). Furthermore, the possibility of timely detecting potential problems in biological wastewater treatment is the main advantage of QIA procedures over standard monitoring techniques (Costa et al., 2013).

This study aims to identify the morphological parameters sensitive to the sludge granulation status and sludge settling properties, using QIA techniques and multivariate statistical analysis, during two granulation processes from activated to granular sludge under different organic loading rates (OLR) and increasing minimal imposed settling velocities.

2. Material and methods

2.1. Reactors set-up and experimental conditions

Two lab-scale SBRs (R1 and R2) with a working volume of 1 L were used in this experiment and operated in parallel with two different OLRs. The reactors dimensions were 9 cm in diameter and 18.5 cm in height. The hydraulic retention time was 12 h, with an exchange ratio of 50 %. Both SBRs were operated in cycles of 6 h, integrating 4 different phases, i.e. anaerobic feed, aeration, settling, and effluent removal. Oxygen was supplied at the bottom of the reactors, resulting in a superficial air velocity of 2 cm s^{-1}, providing complete mixing during the aeration phase and dissolved oxygen saturation in the famine period. The reactors were operated in 3 distinct stages, with increasing minimal imposed sludge settling velocities of 0.27 m h^{-1} (stage I), 0.53 m h^{-1} (stage II), and 5.3 m h^{-1} (stage III). Detailed information is shown in supplementary information (SI) Table S1. The minimal imposed settling velocity was calculated using the following equation (Liu et al., 2005):

$$\text{Minimal imposed settling velocity} = \frac{L}{t_s}$$

where L is the distance to the discharge port (m) and t_s is the settling time (h).

Activated sludge from the municipal wastewater treatment plant of Frossos (Braga, Portugal) was used as inoculum. Both reactors were fed with sodium acetate as sole carbon source, with an OLR of 1.1 ± 0.6 kg_{COD} m^{-3} d^{-1} and 2.0 ± 0.2 kg_{COD} m^{-3} d^{-1} applied in R1 and R2, respectively. Beyond carbon source, 10 mL and 20 mL of a macronutrients stock solution was added (per L^{-1}) to R1 and R2, respectively, with the following composition: $MgSO_4.7H_2O$ (9 g L^{-1}), KCl (4 g L^{-1}), $CaCl_2.2H_2O$ (3 g L^{-1}), NH_4Cl (20 g L^{-1}), K_2HPO_4 (64 g L^{-1}), and KH_2PO_4

(15 g L^{-1}). A volume of 1.5 mL (per L^{-1}) of a concentrated trace solution was added to both reactors with the following composition: $FeCl_3.6H_2O$ 6 g L^{-1}; H_3BO_3 0.6 g L^{-1}; $CuSO_4.5H_2O$ 0.12 g L^{-1}; KI 0.72 g L^{-1}; $MnCl_2.4H_2O$ 0.48 g L^{-1}; $Na_2MoO_2.2H_2O$ 0.24 g L^{-1}; $ZnSO_4.7H_2O$ 0.48 g L^{-1}; $CoCl_2.6H_2O$ 0.6 g L^{-1}, and EDTA 40 g L^{-1}.

2.2. Analytical methods

Mixed liquor volatile suspended solids (MLVSS), effluent volatile suspended solids ($VSS_{effluent}$), and sludge volume index at 5 min (SVI_5) and 30 min (SVI_{30}) were determined according to the Standard Methods (APHA, 2005). Chemical oxygen demand (COD) of both influent and effluent was determined using a COD-cuvette test kit (Hach-Lange GmbH, Dusseldorf, Germany) and DR2800™ spectrophotometer (Hach-Lange, GmbH). The COD concentration available for the aeration period ($COD_{aeration}$) was determined at the transition between anaerobic feeding and aeration phases.

2.3. Quantitative image analysis

2.3.1. Image acquisition

Alongside the determination of the operational parameters, a sample volume of 10 mL was collected for sludge observation at the beginning of the aeration phase, when a complete mixture of the sludge was obtained. Aggregates and filaments images were acquired in bright-field with a 100× magnification using an Olympus BX-51 microscope (Olympus, Shinjuku, Japan) and an Olympus DP71 camera (Olympus, Shinjuku, Japan). For that purpose, a 10 μL sample was placed in a slide by means of a micropipette with a sectioned tip to allow the passage of aggregates, and a cover slip (20 × 20 mm) was positioned on top. This procedure was performed in triplicate for each sample. In order to have representative information about the sludge's morphology, a total of 150 images were acquired per sample (3 × 50 images screened per slide). Images were acquired with cellSens software (Olympus, Shinjuku, Japan), in 1360 × 1024 pixels and 8-bit format.

Granules images were acquired using an Olympus SZ-40 stereo microscope (Olympus, Shinjuku, Japan), with a 15× magnification. Prior to image acquisition, the sludge samples were diluted and granules were let to settle. Floccular sludge in supernatant was discarded and the settled granules were resuspended to its initial volume. For image acquisition, a fixed volume was placed in a Petri dish and all the aggregates present in that volume were captured. This procedure was performed in duplicate. Images were recorded with a CCD AVC D5CE Sony video camera (Sony, Tokyo, Japan) and Image Pro Plus software (Media Cybernetics, MD, USA), in 768 × 576 pixels and 8-bit format.

Typical images acquired at the end of each stage are provided in SI Figure S1.

2.3.2. Image processing and analysis

All aggregates and filaments image processing, including pretreatment, segmentation and debris elimination steps, was performed as described in Mesquita et al. (2016). Binary images were created with the recognized aggregates and free and protruding filamentous bacteria, allowing the subsequent morphological parameters determination (SI Figure S2). All aggregates with Deq < 200 μm were considered flocs, and aggregates with Deq ≥ 200 μm were considered granules (de Kreuk et al., 2007), based on the aggregates area (Area), from which the Deq was calculated:

$$\mathrm{Deq} = 2F_{cal}\sqrt{\frac{Area}{\pi}}$$

where F_{cal} is the calibration factor (μm $pixel^{-1}$). Bright-field microscopy allowed to monitor aggregates with Deq below 650 μm (SI Figure S2ab) since larger aggregates were cut-off by the boundaries (SI Figure S2cd). For that reason, aggregates with Deq above 650 μm were quantified by stereo microscopy (SI Figure S2ef). The sum of all the recognized aggregates area per unit of volume was used to determine the specific area ($Area_{spec}$) for each Deq size range, calculated as follows:

$$Area_{spec} = \frac{\Sigma Area}{Volume}$$

In the case of aggregates quantified by bright-field microscopy, the volume considered was the volume of each image (V_{image}), calculated as follows:

$$H = \frac{V_{sample}}{A_{cover\ slip}}$$

$$V_{image} = H \times A_{image}$$

where, H is the distance between the slide and the cover slip (mm), V_{sample} is the sample volume placed in the slide (mm^3), $A_{cover\ slip}$ is the area of the cover slip (mm^2) and the A_{image} is the area of the image (mm^2) determined using the F_{cal}.

A total of 69 parameters were determined to characterize the aggregates morphology and filaments content during the granulation process (SI Table S2). The morphology of the aggregates within a Deq size range was characterized by several shape descriptors, with the solidity, eccentricity and convexity studied in detail. The aggregates solidity (Sol) was determined as follows:

$$Sol = \frac{Area}{Area_C}$$

where $Area_c$ is the convex envelope area (Amaral, 2003). The aggregates eccentricity (Ecc) was determined as follows:

$$Ecc = \frac{(4\pi)^2\,(M_{2x} - M_{2y})^2 + 4M_{2xy}^2}{Area^2}$$

where M_{2xy} is the second horizontal (x) and vertical (y) orders moment (Amaral, 2003). The aggregates convexity (Conv) was calculated as follows:

$$Conv = \frac{Perimeter_C}{Perimeter}$$

where $Perimeter_c$ is the convex envelope perimeter (Amaral, 2003). More information about the calculation of these parameters can be found in Amaral (2003). The image processing and analysis routines were performed in Matlab™ 8.5 (the MathWorks Inc, USA).

2.4. Multivariate statistical analysis

Principal component analysis (PCA) aims to determine hidden and complex relationships between parameters that compose an X dataset. PCA was performed using the morphological data determined by QIA (SI Table S2). A total of 66 parameters and 40 observations composed the X dataset matrix. Prior to PCA, each variable was scaled as described in Costa et al. (2009). The mathematical principles of PCA can be found in Rosen (2001).

Partial least squares (PLS) regression was performed as described in Mesquita et al. (2016) to predict sludge settling ability (Y), namely SVI_5 and SVI_{30}, using 69 parameters and 40 observations that composed the X dataset matrix (SI Table S2). PLS models were performed independently for each reactor and then combined as the ensemble PLS model (Amaral et al., 2013; Mesquita et al., 2016). Therefore, the overall dataset was divided into two datasets of 69 parameters and 20 observations corresponding to each reactor operation. Each dataset was randomly divided into a training set (67 % of observations) and a validation set (33 % of the observations) to calibrate and validate the model, respectively. To reduce the number of X predictors, a first PLS was performed for each target Y, allowing to determine the variable importance in projection

(VIP) of each predictor of the X dataset. To avoid overfitting, the number of predictors for the second PLS model was equal to $n/2$, with n being the number of observations of the training dataset. Also, whenever two VIP variables exhibited a correlation coefficient above 0.7, the one presenting the lowest VIP value was excluded. Thus, the second PLS was performed using only 6 variables presenting the highest VIP values (SI Table S3). The PLS models root mean square error of prediction (RMSEP) and residual predictive deviation (RPD) were used as the basis of the prediction's accuracy. PCA and PLS principles are detailed in SI and were performed in Matlab™ 8.5 (the MathWorks Inc, USA).

3. Results

3.1. Sludge properties: solids concentration, settling properties and COD depletion

In R1, after an initial washout of 66 % of the inoculated MLVSS, the MLVSS increased steadily during stage I from day 6 to day 27 (Fig. 1a). In R2, 36 % more MLVSS accumulated during stage I, reaching a stable value of 4 g L^{-1} on day 15. Decreasing the settling time in stage II and stage III induced the selection of aggregates with a minimal imposed settling velocity of 0.53 m h^{-1} and 5.3 m h^{-1}, respectively (SI Table S1), with a concomitant change in the MLVSS that oscillated between 2.1 and 3.3 g L^{-1} in R1 and 3.5–4.7 g L^{-1} in R2 during stage II, and a severe, yet transient reduction of about 50 % in the MLVSS concentration in both reactors in stage III (Fig. 1a).

The $VSS_{effluent}$ gradually decreased in both reactors and remained rather stable from day 11 until the end of stage II in R1 though more unstable in R2 (Fig. 1b). Larger fluctuations in $VSS_{effluent}$ in R2 were persistent in stage III, increasing drastically up to 0.45 g L^{-1}, whereas stable values around 0.05 g L^{-1} were observed in R1, after a slight transient increase just after the change of the settling time (Fig. 1b).

The SVI_{30}/SVI_5 rapidly increased in R1 and reached a value of one in the first 6 days of operation, and despite the transient SVI_{30}/SVI_5 decrease observed in stage I, the excellent sludge settling characteristics remained unchanged also after reducing the settling time in stages II and III (Fig. 1c). In R2, the SVI_{30}/SVI_5 oscillated between 0.5 and 0.7 during stage I and II (Fig. 1c) and, albeit the SVI_{30} decreased to values similar to R1 in stage II, SVI_5 was still considerably higher (Fig. 1d). After reducing the settling time in stage III, SVI_5 clearly approached SVI_{30} (Fig. 1e), indicating that the sludge settling ability considerably improved, with the SVI_{30}/SVI_5 reaching values above 0.9, yet with an oscillatory tendency (Fig. 1c).

Both reactors exhibited good COD removal efficiencies throughout all stages (SI Figure S3). The amount of substrate available during the aerobic phase ($COD_{aeration}$) decreased from stage I to stage II in both reactors, indicating an efficient substrate consumption during the anaerobic feeding phase (SI Figure S3). In stage III, when the minimal imposed settling velocity was increased to 5.3 m h^{-1}, an increase in $COD_{aeration}$ was observed in both reactors, though more significant in R2 likely due to the severe washout observed in this reactor in stage III (SI Figure S3).

3.2. QIA as monitoring tool for sludge morphological changes in granulation

3.2.1. Aggregates distribution and filamentous content

The formation and distribution of aggregates revealed differences in the dynamic behaviour between flocs (Deq < 200 μm), granules (Deq ≥ 200 μm), and filamentous bacteria in both reactors (Fig. 2). After 8 days of operation in R1, the $Area_{spec}$ of aggregates with Deq < 200 μm decreased drastically in circa 50% and remained rather stable during stage I (Fig. 2a). In R2, the $Area_{spec}$ of these aggregates gradually increased during stage I and was 1.8x higher at day 27 than in the inoculum (Fig. 2b). The formation of small granules, i.e., with 200 μm ≤ Deq ≤ 650 μm, started after 4 days of operation in both reactors, yet a higher granulation rate was observed in R1 than in R2 (Fig. 2ab). Larger granules with Deq > 650 μm were formed at the lowest minimal

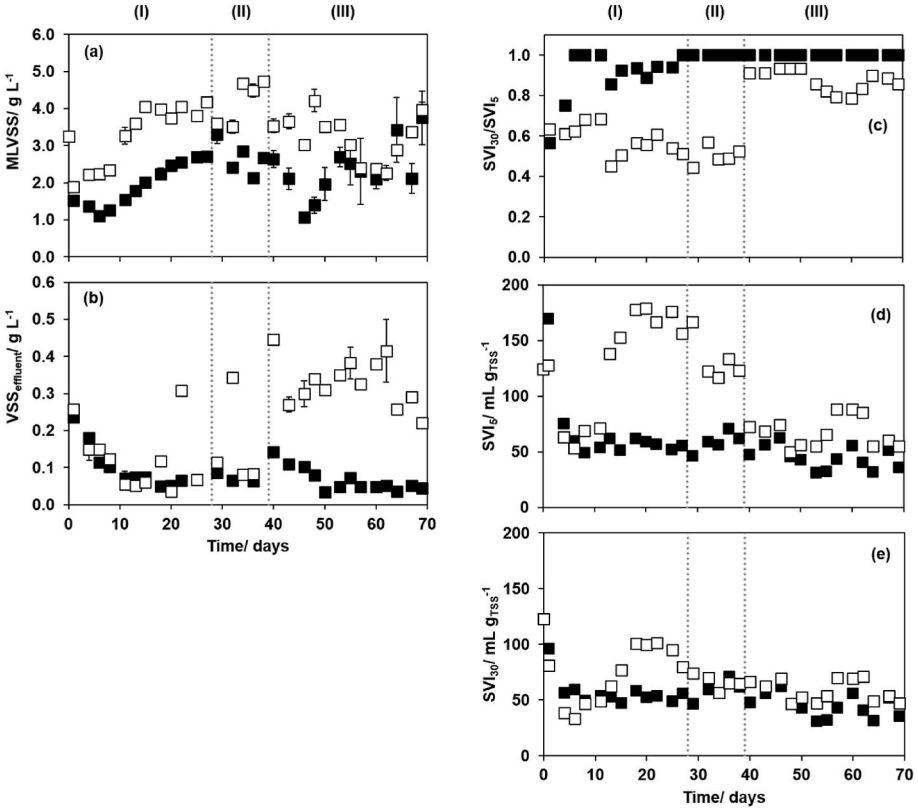

Fig. 1. Sludge profiles of MLVSS (a), $VSS_{effluent}$ (b), SVI_{30}/SVI_5 ratio (c), SVI_5 (d), and SVI_{30} (e) in R1 (■) and R2 (□). Operational stages I, II and III.

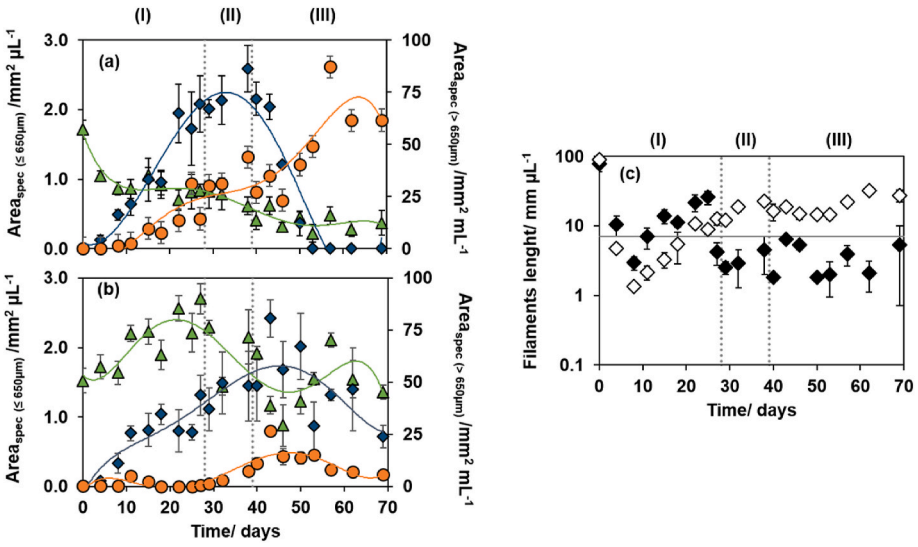

Fig. 2. The specific area of aggregates in the different size range: Deq < 200 µm (▲); 200 µm ≤ Deq ≤ 650 µm (◆) and Deq > 650 µm (●) in R1 (a) and R2 (b). Filaments length (c) in R1 (◆) and R2 (◇) with filaments content threshold of 7 mm µL^{-1} (——), according to Mesquita (2010). Operational stages I, II, III.

imposed settling velocity (0.27 m h^{-1}; stage I), but only in R1 and after day 15 (Fig. 2a). In R1, from day 38–50, the increase of the minimal imposed settling velocity to 5.3 m h^{-1} (stage III) induced a significant increase of the Area$_{spec}$ of granules with Deq > 650 µm, more pronounced from day 46 onwards, revealing the maturation of granules in R1 (Fig. 2a). This was simultaneous with the decrease in the Area$_{spec}$ of granules with 200 µm ≤ Deq ≤ 650 µm from 2.6 ± 0.3 mm^2 µL^{-1} to 0.4 ± 0.2 mm^2 µL^{-1} in the same period (Fig. 2a). Conversely in R2, the Area$_{spec}$ of granules with 200 µm ≤ Deq ≤ 650 µm continued its increasing trend during stage II and part of stage III (Fig. 2b), and granules with Deq > 650 µm started to accumulate in the same period, but well below the values observed in R1 (Fig. 2ab). Simultaneously, the Area$_{spec}$ of flocs decreased about 60 % with the increase in the minimal imposed settling velocity. Yet from day 46, concomitant with the biomass washout, the flocs Area$_{spec}$ started to fluctuate and increase, opposite to the granules counterpart, revealing the instability of the granulation process in R2 in that period (Fig. 2b).

Most filamentous bacteria present in the inoculum were washed-out in the first 8 days of operation (Fig. 2c). The filament length, of both protruding and free filaments, was higher in R1 than in R2 during most of stage I. Throughout stage II and III, the filament length continued to increase in R2, reaching a maximum of 33 ± 3 mm µL^{-1} at day 62, which was 15x higher than the filaments length quantified in R1 (Fig. 2c).

3.2.2. Morphology characterization of granules with 200 µm ≤ Deq ≤ 650 µm

The morphology of the small granules, i.e., with 200 µm ≤ Deq ≤ 650 µm revealed major differences between the two reactors, related with the distinct granulation rates. Initially, the granules exhibited a low solidity elongated structure (high eccentricity values) and somewhat irregular boundaries (low convexity values) as presented in Fig. 3. In R1, the granules became progressively more compact (increasing solidity values), circular (decreasing eccentricity values) and smooth (increasing convexity values) throughout the reactor operation (Fig. 3 abc). In R2, the structure of the granules remained rather stable throughout stage I, and structural changes were only observed after decreasing the settling time in stage II and III, particularly in terms of solidity and convexity which increased until day 46 (Fig. 3ac). From that day onwards, the granules loss of structural integrity in R2 was evidenced by the gradual decrease in both solidity and convexity and increase in eccentricity (Fig. 3).

3.3. Multivariate statistical analysis

3.3.1. PLS

A PLS analysis was performed to predict SVI$_5$ and SVI$_{30}$ using exclusively QIA data (Fig. 4). The regression analysis between the predicted and observed (measured) values presented good prediction abilities with correlation coefficients (R^2) of 0.9637 and 0.842 for SVI$_5$ and SVI$_{30}$, respectively (Fig. 4). The RMSEP of both models was low for both SVI$_5$ (7.6 mL g_{TSS}^{-1}) and SVI$_{30}$ (5.2 mL g_{TSS}^{-1}), representing 5.2 % and 5.6 % of the values range observed for SVI$_5$ and SVI$_{30}$, respectively (Fig. 4). The RPD values for both PLS models were 5.57 and 4.12 for SVI$_5$ and SVI$_{30}$, respectively, above the value 3 considered to be the threshold for a satisfactory prediction (Cozzolino et al., 2004). The assessment of SVI$_5$ and SVI$_{30}$, depended on a relatively similar set of variables, both for R1 and for R2 (SI Table S3). Indeed, 5 out of the 6 main morphological parameters employed for both SVI predictions in R1 were the same, encompassed within the filamentous bacteria, overall aggregates, granules size, and flocs morphology. On the other hand, 4 out of the 6 main morphological parameters employed for the SVI predictions in R2 were also similar, comprised within the overall aggregates, granules size, and flocs morphology.

3.3.2. PCA

A PCA was performed due to the large amount of data generated by QIA determining, for each principal component (PC), the scores containing information on how the samples points are related to each other, and the loadings establishing the influence of each variable on the PC (Fig. 5). The two most relevant PC (PC1 and PC2) given by PCA, explained 68.7 % of the dataset variance and were used in this analysis. In Fig. 5a it is possible to observe 4 main clusters, corresponding to the morphological changes of the seed AS throughout the reactors operation. The first cluster (C1), located at the top left quadrant with high scores in PC2, incorporates the initial inoculum for both reactors (day 0), and the second (C2), third (C3) and fourth (C4) clusters encompass the remaining sludge observations of R1 and R2 (Fig. 5a). PC1 allowed to clearly distinguish C1 from C4 and both from C2 and C3 clusters, whereas PC2 allowed to distinguish the C2 and C3 clusters. The C2 cluster was situated in the top right corner (high PC1 and PC2 values)

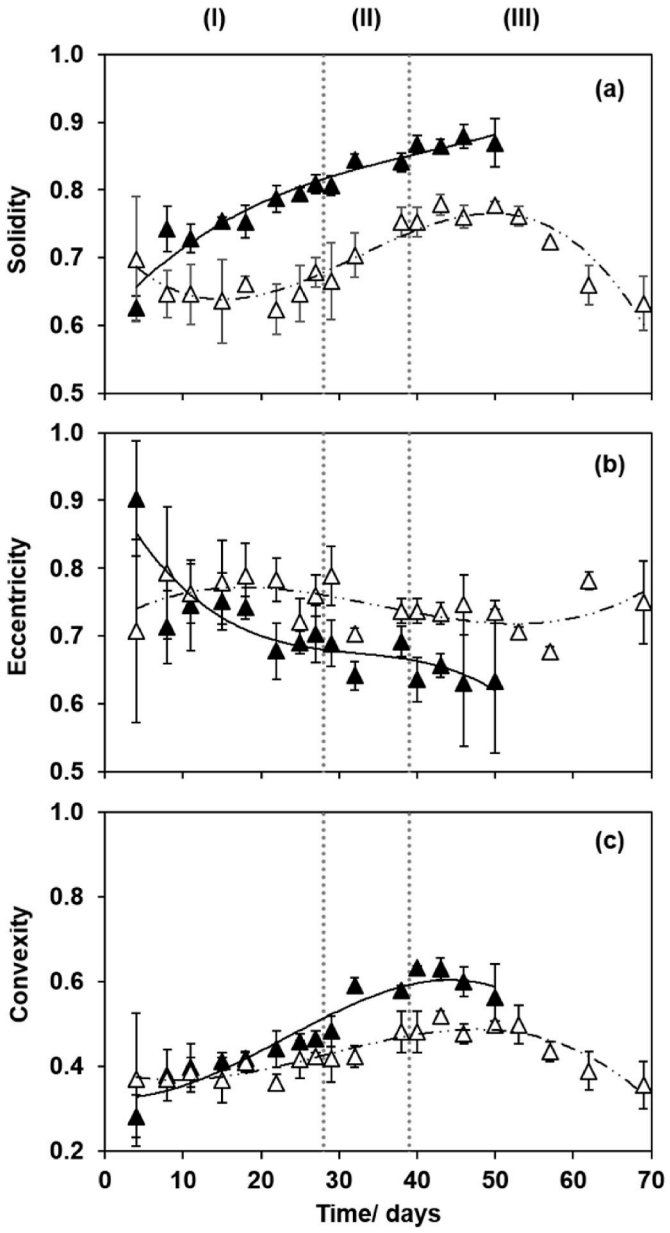

Fig. 3. –The solidity (a), eccentricity (b), and convexity (c) of aggregates with 200 μm ≤ Deq ≤ 650 μm present in R1 (▲) and R2 (△), during the operational stages I, II and III.

which, according to Fig. 5b, is positively influenced by the parameters related mainly with the morphology and prevalence of the aggregates below 200 μm (and between 200 μm and 650 μm at some extent). Thus, it can be implied that the C2 cluster was related with the first development of the inoculum toward the obtainment of a granular structure (Fig. 5ab). On the other hand, the C3 cluster differed from the C2 cluster by shifting mostly along the PC2 axis (Fig. 5a) towards negative PC2 values. The parameters that negatively influenced PC2 were mostly related with the morphology and prevalence of granules with 200 μm ≤ Deq ≤ 650 μm. A transient shift toward the C3 cluster could be observed in R2 (days 43, 46 and 50), corresponding to an increase amount of these granules. However, such trend did not endure, with the subsequent points again being allocated to the C2 cluster (in accordance with the biomass washout and instability in R2). On the other hand, most R1 observations fell within the C3 cluster, though, from day 50 onwards moved back (negatively) in the PC1 axis, influenced by the granules maturation process. Indeed, the 3 final observations (days 57, 62 and 69) formed the C4 cluster located in the top left quadrant (Fig. 5a), which can find a parallel to the fact that PC1 is negatively influenced by the parameters related with the morphology and prevalence of the larger granules (Deq > 650 μm).

4. Discussion

Faster granulation is often reported in AGS systems treating wastewater at high OLR, however, the resulting granules are usually unstable and granule disruption is often observed (Liu and Tay, 2015; Val Del Río et al., 2013). Stable granules are usually obtained at low OLR (≤ 2.0 kgCOD m^{-3} d^{-1}), commonly found in CAS systems (Franca et al., 2018). One major disadvantage is the extended period of time required for granulation, monitored by the dynamic sludge settling behaviour (Pronk et al., 2015b), even though the treatment requirements in full-scale AGS systems can be achieved prior to the completion of the granulation process.

The gradual decrease of the settling time, which determines the minimal imposed settling velocity, is commonly applied to select fast settling granules over slow settling flocs, influencing the granulation rate. However, establishing a turning point based on sludge properties and qualitative observations, is extremely ambiguous, since granulation is a transient process of gradual morphological changes from flocs to granules (Liu et al., 2010). Both floccular and granular sludge are expected to coexist even after the granulation is completed, hence, monitoring the sludge morphology of flocs and granules, as well as the filamentous bacteria proliferation could help understanding the sludge tendency to granulate at an early stage of the process and monitor the process stability overtime. More importantly, collecting precise and quantitative morphological information about how the granulation process occurs in different operating conditions is relevant to the academic and technical communities in predicting granulation rates and

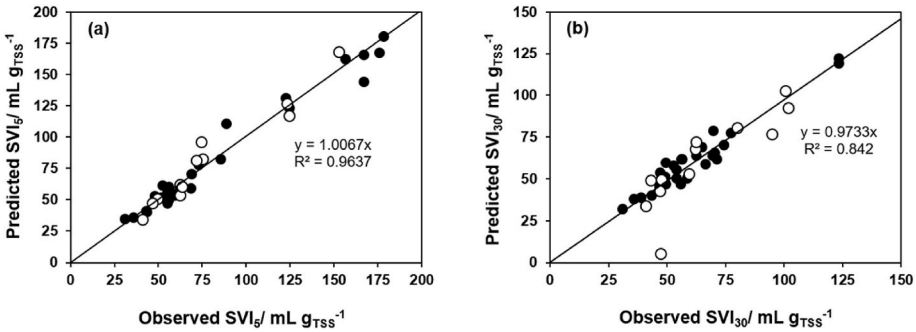

Fig. 4. Correlation between observed and predicted SVI_5 (a) and SVI_{30} (b). Calibration (●) and validation (○) data set.

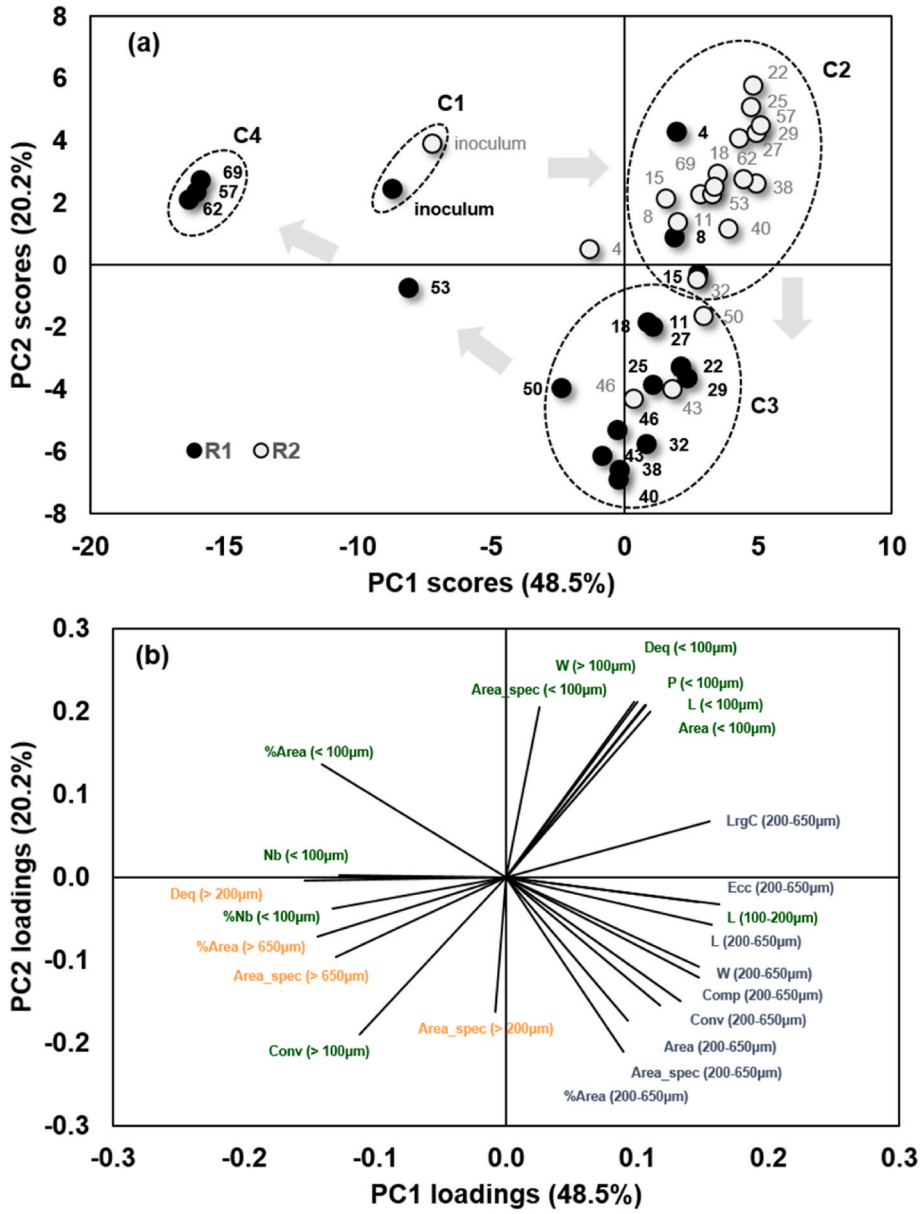

Fig. 5. PCA scores plot of the QIA dataset for PC1 vs PC2 (a) of R1 (●) and R2 (○). Variables loadings plot of the PC1 and PC2 (b).

granule stability. In accordance, a QIA technique was used in this study to monitor and quantify the sludge morphological differences and evolution in both reactors during the granulation process.

The performed sludge monitoring allowed to infer the start of the granulation process in R1 during stage I, were it reached a stable MLVSS concentration and good settling properties. On the other hand, in R2, good settling properties were attained only after the increase of the minimal imposed settling velocity to 5.3 m h^{-1} in stage III, thus suggesting a slower granulation process. QIA data evidenced that the operating conditions applied to R1 and R2 were effective to promote the formation and accumulation of granules. In both reactors the granulation started at the minimal imposed settling velocity of 0.27 m h^{-1}, with the formation and accumulation of small granules with 200 µm ≤ Deq ≤ 650 µm after 4 days (Fig. 2ab). Nevertheless, the granulation process was evidently slower in R2 which had a higher organic load applied. Previous works have shown that high OLR (up to 12 kg_{COD} m^{-3} d^{-1}) can be used as a strategy to speed up the granulation start-up process when combined with strong hydraulic selective pressures (Liu and Tay, 2015). Thus, while the minimal imposed settling velocity of 0.27 m h^{-1} promoted microbial aggregation in R2 at an early stage of the operation, only after the increase of the minimal imposed settling velocity to 0.53 m h^{-1} and later to 5.3 m h^{-1} the formation of larger granules (Deq > 650 µm) was induced (though still to a lower degree than in RI), evidencing that a higher selective pressure was required to stimulate the granulation process. However, the granulation in R2 was rather unstable and transitory leading to biomass and granules washout at the end of the operation. In R1, a strong increase of granules with Deq > 650 µm was observed after the increase of the minimal imposed settling velocity to 5.3 m h^{-1}, leading to mature granules, particularly from day 46 onwards (Fig. 2a). This was due possibly to the increase of the food to microorganisms ratio (F/M) (SI Figure S4), since high F/M influences the formation of larger granules (Li et al., 2011).

Throughout the granulation process in R1, the SVI_5 equalled SVI_{30}, considered an indication of full granulation (Liu and Tay, 2007), just after 6 days when granules were far from being predominant in terms of $Area_{spec}$ (Fig. 2a). However, studies performed in pilot-scale have shown SVI_{30}/SVI_5 values above 0.9 for AGS while still dominated by flocs (Liu et al., 2010). And, although in this study the SVI_{30}/SVI_5 ratio did not

reveal the degree of granulation in the reactors, the decrease of both SVI_5 and SVI_{30} in R1 was consistent with the decrease of the flocs $Area_{spec}$. On the other hand, the floccular sludge decrease was not so prominent in R2, with the inefficient withdrawal of the slow settling aggregates sustaining the gradual increase of SVI_5 and SVI_{30} throughout stage I and potentially delayed the granulation process in this reactor (Beun et al., 1999). The reason behind the prevalence of flocs in R2 seems to be related with sludge aggregation and disruption phenomena, as shown by the distinct morphology of the granules with 200 μm ≤ Deq ≤ 650 μm in both reactors.

The use of granules morphological parameters, such as aspect ratio and shape factor, for monitoring the granulation process has already been employed by Beun et al. (2002). These parameters increased in the first 10 days of the operation, remaining stable throughout the remaining timespan even after transitory disruption. In our work, while the evolution in the granules morphology in R1 evidenced a progressively stronger structure throughout the granulation process, the R2 granules lower solidity and convexity, and higher eccentricity, reflected disturbances in the granulation process and may have been indirectly related to the higher presence of flocs. Furthermore, the structural changes evidenced by the shape descriptors from day 29 to day 46 in R2 suggest a stronger microbial aggregation, leading to the formation and accumulation of larger granules (Deq > 650 μm) in the same period. Conversely, after 46 days, the shape descriptors revealed a progressive granules disruption and washout correlated with the flocs increase and higher suspended solids in the effluent ($VSS_{effluent}$).

According to Mesquita (2010), a filamentous bacteria content threshold of 7 mm μL^{-1} was found below which filaments are irrelevant to the sludge settling ability. In R1, the decrease in SVI_{30}/SVI_5 value observed from day 11–25 in stage I was concomitant with the increase of protruding and free filamentous bacteria content above 7 mm μL^{-1} in the same period (Figs. 1c and 2c). Indeed, after day 25, the protruding and free filamentous bacteria content remained below 7 mm μL^{-1} reflecting the constant SVI_{30}/SVI_5 ratio. In R2, the free and protruding filaments content rose above 7 mm μL^{-1} at the end of stage I and remained higher throughout stage II and III, affecting the settling ability of the sludge. Also, the increase of filaments content during stage III is in accordance with the instability of the granules structure in this period.

Several works have reported a clear relation between QIA data and sludge settling ability in CAS systems (Amaral et al., 2013; Amaral and Ferreira, 2005; Grijspeerdt and Verstraete, 1997), though this relation was yet to be proven during a granulation process. In accordance, the current study allowed to advance in this assumption, with the PLS analysis performed with QIA data achieving a high correlation regression (R^2 0.964) between the predicted and observed SVI_5. Even though a good correlation regression (R^2 0.842) between the predicted and observed SVI_{30} was also found, it was evidently lower than for SVI_5, evidencing a deeper complex relation between the sludge morphological changes during granulation and the sludge settling behaviour. For both R1 and R2, the main parameters found most adequate to predict the sludge settling ability encompassed the aggregates, granules size and flocs morphology (SI Table S3). It is known that the aggregates play a defining role in the sludge (both granular and floccular) settling ability (Amaral et al., 2013; Leal et al., 2020). However, a noticeable difference between the sludge settling ability prediction in the two reactors was the fact that, a clear dependency on the filamentous bacteria was found in R1. It may be assumed that high settling ability is obtained for sludge presenting good granular properties (i.e. R1), and the growth of filamentous bacteria lead to changes in the settling properties, thus assuming larger importance in prediction models. On the other hand, for sludge presenting poor granular properties (i.e. R2), the SVI is mainly dependent on the aggregates size, morphology and lesser with the growth of filamentous bacteria. To construct a generalized PLS model able to be applied in all granulation processes is very complex and involves gathering a vast number of observations in distinct conditions. However, care should be taken not to force a single unified and less adapted solution that would not be as accurate for that particular system and let each PLS model address the specificities of the system studied. Therefore, given the complexity and diversity of AGS systems, the PLS flexibility on determining the most significant parameters for each system, can be considered an advantage.

PCA has been already used to identify several activated sludge disturbances through the combination of morphological and physiological data (Mesquita et al., 2011b). More recently, PCA was used to identify the variables associated with the hindered settling velocity of activated sludge in the presence of ferric chloride precipitates (Asensi et al., 2019). Here, the use of PCA in the QIA data allowed to study the evolution of the different phases of the granulation process in both reactors.

Several hypothesis exist regarding the mechanism behind granules formation, such as floccular aggregation (Verawaty et al., 2012), microbial outgrowth from a single microcolony (Barr et al., 2010), or by newly germinated fungal spores (Sarma and Tay, 2018). However, there is no consensus due to the lack of supporting and clear evidences (Sarma and Tay, 2018; Wilén et al., 2018). In this study, the use of PCA with the QIA data allowed to clearly distinguish 4 main clusters associated with the different phases of the granulation process. Cluster C2 (most R2 observations) was formed in the initial stages of the granulation process, and the distinction to the inoculum cluster was mainly due to the morphology and prevalence of the aggregates below 200 μm, evidencing the initial flocs aggregation into larger structures. It seems reasonable to assume that, in this step, variations in the aggregates size and morphology are expected to occur. The distinction between clusters C2 and C3 (most R1 observations) reflected these changes, driven by the evolution towards a granular sludge, as reflected by the relation of the morphology and prevalence of the granules with 200 μm ≤ Deq ≤ 650 μm. The granulation process is assumed to continue by a maturation step, in which, the growth of the immobilized biomass, EPS production and hydrodynamic shear shapes the form of the granules (Sarma et al., 2017). This seemed to be the case with the final data points of R1 which formed the cluster C4, mainly influenced by the size and predominance of larger granules with Deq > 650 μm which reflects the granules maturation. Therefore, the distinct granulation status of both systems could be established overtime from the use of a PCA with the QIA data. This allowed to follow the granulation process, enlightening the differences between the two operating strategies and, thus, being able to anticipate process instability.

In conclusion, the granulation rate heavily depended on the substrate concentration alongside the minimal imposed sludge settling velocity. In R1 (1.1 ± 0.6 kg_{COD} m^{-3} d^{-1}) a good granulation ability could be obtained right from the minimal imposed settling velocity. On the other hand, only at higher minimal imposed settling velocities (and mainly at 5.3 m h^{-1}) granulation leading to larger granules (Deq > 650 μm) was observed in R2 (2.0 ± 0.2 kg_{COD} m^{-3} d^{-1}), yet at a lower extension than in R1. Larger granules accounted for 96.1 % and 9.4 % in term of $Area_{spec}$ of the granular fraction in R1 and R2, respectively. The morphological differences (solidity, eccentricity and convexity) of the small granules (200 μm ≤ Deq ≤ 650 μm) reflected the degree of sludge aggregation and could be used as indicators in the effort to anticipate process instability. Good settling properties were achieved with both OLR, with SVI_5 below 40 mL g_{TSS}^{-1} and 60 mL g_{TSS}^{-1} in R1 and R2, respectively. The sludge morphological data was successfully used to predict the sludge settling properties (SVI_5 and SVI_{30}) by PLS regression, with a correlation coefficient of 0.964 and 0.842 for SVI_5 and SVI_{30}, respectively. Finally, the distinct granulation status of both systems overtime could be established from the use of a PCA with the QIA data, allowing to follow the granulation process, which, in conjunction with the use of the PLS models allows for a timely detection of potential problems.

Author contribution

Sérgio A. Silva: Conceptualization, Investigation, Formal analysis,

Writing – Original draft preparation **Angeles Val del Río:** Investigation, Formal analysis, Writing – Review & editing **António L. Amaral:** Software, Writing – Review & editing **Eugénio C. Ferreira:** Resources, Funding acquisition, Writing – Review & editing **M. Madalena Alves:** Resources, Supervision, Funding acquisition, Writing – Review & editing **Daniela P. Mesquita:** Conceptualization, Resources, Supervision, Writing – Review & editing.

Declaration of competing interest

The authors declare that they have no known competing financial interests or personal relationships that could have appeared to influence the work reported in this paper.

Acknowledgments

The authors thank the Portuguese Foundation for Science and Technology (FCT) under the scope of the strategic funding of UIDB/04469/2020 unit and the project AGeNT PTDC/BTA-BTA/31264/2017 (POCI-01-0145-FEDER-031264). The authors also acknowledge the financial support to Sérgio Alves da Silva through the grant SFRH/BD/122623/2016 provided by FCT. A. Val del Rio is supported by Xunta de Galicia (ED418B 2017/075) and program Iacobus (2018/2019).

Appendix A. Supplementary data

Supplementary data to this article can be found online at https://doi.org/10.1016/j.chemosphere.2021.131637.

References

Amaral, A.L., Ferreira, E.C., 2005. Activated sludge monitoring of a wastewater treatment plant using image analysis and partial least squares regression. Anal. Chim. Acta 544, 246–253. https://doi.org/10.1016/j.aca.2004.12.061.

Amaral, A.L., Mesquita, D.P., Ferreira, E.C., 2013. Automatic identification of activated sludge disturbances and assessment of operational parameters. Chemosphere 91, 705–710. https://doi.org/10.1016/j.chemosphere.2012.12.066.

Amaral, A.L., Pereira, M.A., Da Motta, M., Pons, M.N., Mota, M., Ferreira, E.C., Alves, M. M., 2004. Development of image analysis techniques as a tool to detect and quantify morphological changes in anaerobic sludge: II. Application to a granule deterioration process triggered by contact with oleic acid. Biotechnol. Bioeng. 87, 194–199. https://doi.org/10.1002/bit.20129.

Amaral, A.L.P., 2003. Image Analysis in Biotechnological Processes: Applications to Wastewater Treatment. PhD thesis, University of Minho. http://hdl.handle.net/1822/4506.

APHA, 2005. Standard methods for the examination of water & wastewater. Am. Public Heal. Assoc. Am. Water Work. A ssociation, Water Environ. Fed twenty-first ed.

Araya-Kroff, P., Amaral, A.L., Neves, L., Ferreira, E.C., Pons, M.N., Mota, M., Alves, M.M., 2004. Development of image analysis techniques as a tool to detect and quantify morphological changes in anaerobic sludge: I. Application to a granulation process. Biotechnol. Bioeng. 87, 184–193. https://doi.org/10.1002/bit.20207.

Asensi, E., Zambrano, D., Alemany, E., Aguado, D., 2019. Effect of the addition of precipitated ferric chloride on the morphology and settling characteristics of activated sludge flocs. Separ. Purif. Technol. 227, 115711. https://doi.org/10.1016/j.seppur.2019.115711.

Barr, J.J., Cook, A.E., Bond, P.L., 2010. Granule formation mechanisms within an aerobic wastewater system for phosphorus removal. Appl. Environ. Microbiol. 76, 7588–7597. https://doi.org/10.1128/AEM.00864-10.

Beun, J., Hendriks, A., van Loosdrecht, M.C., Morgenroth, E., Wilderer, P., Heijnen, J., 1999. Aerobic granulation in a sequencing batch reactor. Water Res. 33, 2283–2290. https://doi.org/10.1016/S0043-1354(98)00463-1.

Beun, J.J., Van Loosdrecht, M.C.M., Heijnen, J.J., 2002. Aerobic granulation in a sequencing batch airlift reactor. Water Res. 36, 702–712. https://doi.org/10.1016/S0043-1354(01)00250-0.

Carrera, P., Mosquera-Corral, A., Méndez, R., Campos, J.L., Val del Rio, A., 2019. Pulsed aeration enhances aerobic granular biomass properties. Biochem. Eng. J. 149, 107244. https://doi.org/10.1016/j.bej.2019.107244.

Costa, J.C., Abreu, A.A., Ferreira, E.C., Alves, M.M., 2007. Quantitative image analysis as a diagnostic tool for monitoring structural changes of anaerobic granular sludge during detergent shock loads. Biotechnol. Bioeng. 98, 60–68. https://doi.org/10.1002/bit.21381.

Costa, J.C., Alves, M.M., Ferreira, E.C., 2009. Principal component analysis and quantitative image analysis to predict effects of toxics in anaerobic granular sludge. Bioresour. Technol. 100, 1180–1185. https://doi.org/10.1016/j.biortech.2008.09.018.

Costa, J.C., Mesquita, D.P., Amaral, A.L., Alves, M.M., Ferreira, E.C., 2013. Quantitative image analysis for the characterization of microbial aggregates in biological wastewater treatment: a review. Environ. Sci. Pollut. Res. 20, 5887–5912. https://doi.org/10.1007/s11356-013-1824-5.

Cozzolino, D., Kwiatkowski, M.J., Parker, M., Cynkar, W.U., Dambergs, R.G., Gishen, M., Herderich, M.J., 2004. Prediction of phenolic compounds in red wine fermentations by visible and near infrared spectroscopy. Anal. Chim. Acta 513, 73–80. https://doi.org/10.1016/j.aca.2003.08.066.

de Kreuk, M.K., Kishida, N., van Loosdrecht, M.C.M., 2007. Aerobic granular sludge - state of the art. Water Sci. Technol. 55, 75–81. https://doi.org/10.2166/wst.2007.244.

Devlin, T.R., di Biase, A., Kowalski, M., Oleszkiewicz, J.A., 2017. Granulation of activated sludge under low hydrodynamic shear and different wastewater characteristics. Bioresour. Technol. 224, 229–235. https://doi.org/10.1016/j.biortech.2016.11.005.

Franca, R.D.G., Pinheiro, H.M., van Loosdrecht, M.C.M., Lourenço, N.D., 2018. Stability of aerobic granules during long-term bioreactor operation. Biotechnol. Adv. 36, 228–246. https://doi.org/10.1016/j.biotechadv.2017.11.005.

Grijspeerdt, K., Verstraete, W., 1997. Image analysis to estimate the settleability and concentration of activated sludge. Water Res. 31, 1126–1134. https://doi.org/10.1016/S0043-1354(96)00350-8.

Jiang, Y., Shi, X., Ng, H.Y., 2021. Aerobic granular sludge systems for treating hypersaline pharmaceutical wastewater: start-up, long-term performances and metabolic function. J. Hazard Mater. 412, 125229. https://doi.org/10.1016/j.jhazmat.2021.125229.

Leal, C., Val del Río, A., Ferreira, E.C., Mesquita, D., Amaral, A.L., 2021b. Validation of a quantitative image analysis methodology for the assessment of the morphology and structure of aerobic granular sludge in the presence of pharmaceutically active compounds. Environ. Technol. Innov. 23, 101639. https://doi.org/10.1016/j.eti.2021.101639.

Leal, C., Val del Río, A., Mesquita, D.P., Amaral, A.L., Castro, P.M.L., Ferreira, E.C., 2020. Sludge volume index and suspended solids estimation of mature aerobic granular sludge by quantitative image analysis and chemometric tools. Separ. Purif. Technol. 234, 116049. https://doi.org/10.1016/j.seppur.2019.116049.

Leal, C.S., Lopes, M., Val del Río, A., Quintelas, C., Castro, P.M.L., Ferreira, E.C., Amaral, A.L., Mesquita, D.P., 2021a. Assessment of an aerobic granular sludge system in the presence of pharmaceutically active compounds by quantitative image analysis and chemometric techniques. J. Environ. Manag. 289, 112474. https://doi.org/10.1016/j.jenvman.2021.112474.

Li, A.J., Li, X.Y., Yu, H.Q., 2011. Effect of the food-to-microorganism (F/M) ratio on the formation and size of aerobic sludge granules. Process Biochem. 46, 2269–2276. https://doi.org/10.1016/j.procbio.2011.09.007.

Li, A.J., Yang, S.F., Li, X.Y., Gu, J.D., 2008. Microbial population dynamics during aerobic sludge granulation at different organic loading rates. Water Res. 42, 3552–3560. https://doi.org/10.1016/j.watres.2008.05.005.

Liu, J., Li, J., Wang, X., Zhang, Q., Littleton, H., 2017. Rapid aerobic granulation in an SBR treating piggery wastewater by seeding sludge from a municipal WWTP. J. Environ. Sci. (China) 51, 332–341. https://doi.org/10.1016/j.jes.2016.06.012.

Liu, Y., Tay, J.-H., 2002. The essential role of hydrodynamic shear force in the formation of biofilm and granular sludge. Water Res. 36, 1653–1665. https://doi.org/10.1016/S0043-1354(01)00379-7.

Liu, Y., Wang, Z.W., Tay, J.H., 2005. A unified theory for upscaling aerobic granular sludge sequencing batch reactors. Biotechnol. Adv. 23, 335–344. https://doi.org/10.1016/j.biotechadv.2005.04.001.

Liu, Y.Q., Moy, B., Kong, Y.H., Tay, J.H., 2010. Formation, physical characteristics and microbial community structure of aerobic granules in a pilot-scale sequencing batch reactor for real wastewater treatment. Enzym. Microb. Technol. 46, 520–525. https://doi.org/10.1016/j.enzmictec.2010.02.001.

Liu, Y.Q., Tay, J.H., 2015. Fast formation of aerobic granules by combining strong hydraulic selection pressure with overstressed organic loading rate. Water Res. 80, 256–266. https://doi.org/10.1016/j.watres.2015.05.015.

Liu, Y.Q., Tay, J.H., 2007. Characteristics and stability of aerobic granules cultivated with different starvation time. Appl. Microbiol. Biotechnol. 75, 205–210. https://doi.org/10.1007/s00253-006-0797-4.

Mesquita, D., 2010. Image Analysis and Chemometric Tools to Characterize Aggregated and Filamentous Bacteria in Activated Sludge Process. PhD thesis. University of Minho. http://hdl.handle.net/1822/12470.

Mesquita, D.P., Amaral, A.L., Ferreira, E.C., 2016. Estimation of effluent quality parameters from an activated sludge system using quantitative image analysis. Chem. Eng. J. 285, 349–357. https://doi.org/10.1016/j.cej.2015.09.110.

Mesquita, D.P., Amaral, A.L., Ferreira, E.C., 2011a. Identifying different types of bulking in an activated sludge system through quantitative image analysis. Chemosphere 85, 643–652. https://doi.org/10.1016/j.chemosphere.2011.07.012.

Mesquita, D.P., Amaral, A.L., Ferreira, E.C., 2011b. Characterization of activated sludge abnormalities by image analysis and chemometric techniques. Anal. Chim. Acta 705, 235–242. https://doi.org/10.1016/j.aca.2011.05.050.

Morgenroth, E., Sherden, T., Van Loosdrecht, M.C.M., Heijnen, J.J., Wilderer, P.A., 1997. Aerobic granular sludge in a sequencing batch reactor. Water Res. 31, 3191–3194. https://doi.org/10.1016/S0043-1354(97)00216-9.

Pronk, M., Abbas, B., Al-zuhairy, S.H.K., Kraan, R., Kleerebezem, R., van Loosdrecht, M. C.M., 2015a. Effect and behaviour of different substrates in relation to the formation of aerobic granular sludge. Appl. Microbiol. Biotechnol. 99, 5257–5268. https://doi.org/10.1007/s00253-014-6358-3.

Pronk, M., de Kreuk, M.K., de Bruin, B., Kamminga, P., Kleerebezem, R., van Loosdrecht, M.C.M., 2015b. Full scale performance of the aerobic granular sludge process for sewage treatment. Water Res. 84, 207–217. https://doi.org/10.1016/j.watres.2015.07.011.

Rollemberg, S.L. de S., Barros, A.R.M., de Lima, J.P.M., Santos, A.F., Firmino, P.I.M., dos Santos, A.B., 2019. Influence of sequencing batch reactor configuration on aerobic granules growth: engineering and microbiological aspects. J. Clean. Prod. 238 https://doi.org/10.1016/j.jclepro.2019.117906.

Rosen, C., 2001. A Chemometric Approch to Process Monitoring and Control with Application to Wastewater Treatment Operation, PhD Thesis. Lund University.

Sarma, S.J., Tay, J.H., 2018. Aerobic granulation for future wastewater treatment technology: challenges ahead. Environ. Sci. Water Res. Technol. 4, 9–15. https://doi.org/10.1039/c7ew00148g.

Sarma, S.J., Tay, J.H., Chu, A., 2017. Finding knowledge gaps in aerobic granulation technology. Trends Biotechnol. 35, 66–78. https://doi.org/10.1016/j.tibtech.2016.07.003.

Sguanci, S., Lubello, C., Caffaz, S., Lotti, T., 2019. Long-term stability of aerobic granular sludge for the treatment of very low-strength real domestic wastewater. J. Clean. Prod. 222, 882–890. https://doi.org/10.1016/j.jclepro.2019.03.061.

Su, K.Z., Yu, H.Q., 2005. Formation and characterization of aerobic granules in a sequencing batch reactor treating soybean-processing wastewater. Environ. Sci. Technol. 39, 2818–2827. https://doi.org/10.1021/es048950y.

Val Del Río, A., Figueroa, M., Mosquera-Corral, A., Campos, J.L., Méndez, R., 2013. Stability of aerobic granular biomass treating the effluent from a seafood industry. Int. J. Environ. Res. 7, 265–276. https://doi.org/10.22059/ijer.2013.606.

Verawaty, M., Pijuan, M., Yuan, Z., Bond, P.L., 2012. Determining the mechanisms for aerobic granulation from mixed seed of floccular and crushed granules in activated sludge wastewater treatment. Water Res. 46, 761–771. https://doi.org/10.1016/j.watres.2011.11.054.

Wagner, J., Weissbrodt, D.G., Manguin, V., Ribeiro da Costa, R.H., Morgenroth, E., Derlon, N., 2015. Effect of particulate organic substrate on aerobic granulation and operating conditions of sequencing batch reactors. Water Res. 85, 158–166. https://doi.org/10.1016/j.watres.2015.08.030.

Wilén, B.M., Liébana, R., Persson, F., Modin, O., Hermansson, M., 2018. The mechanisms of granulation of activated sludge in wastewater treatment, its optimization, and impact on effluent quality. Appl. Microbiol. Biotechnol. 102, 5005–5020. https://doi.org/10.1007/s00253-018-8990-9.

Xavier, J.A., Guimarães, L.B., Magnus, B.S., Leite, W.R., Vilar, V.J.P., da Costa, R.H.R., 2021. How volumetric exchange ratio and carbon availability contribute to enhance granular sludge stability in a fill/draw mode SBR treating domestic wastewater? J. Water Process Eng. 40 https://doi.org/10.1016/j.jwpe.2021.101917.

Zhang, B., Ji, M., Qiu, Z., Liu, H., Wang, J., Li, J., 2011. Microbial population dynamics during sludge granulation in an anaerobic-aerobic biological phosphorus removal system. Bioresour. Technol. 102, 2474–2480. https://doi.org/10.1016/j.biortech.2010.11.017.